Search for Gauge-Mediated Supersymmetry-Breaking Events in the $\gamma\gamma$+Missing Transverse Energy Final State at CDF II

(Dated: July 6, 2009; Version 0.3; Line-count 495 out of 460)

We present the results of search for a gauge-mediated supersymmetry-breaking events with $\widetilde{\chi}_1^0 \rightarrow \gamma\widetilde{G}$ in the $\gamma\gamma$+missing transverse energy final state. In 2.6$\pm$0.2 fb^{-1} of $p\bar{p}$ collisions at $\sqrt{s} = 1.96$ TeV recorded by the CDF II detector we observe no candidate events, consistent with a standard model background expectation of 1.4$\pm$0.4 events. We set 95% C.L. cross section limits and place a world-best limit on the $\widetilde{\chi}_1^0$ mass of 149 GeV/c^2 at $\tau_{\tilde{\chi}_1^0}$= 0 ns as well as make exclusions in the $\widetilde{\chi}_1^0$ mass-lifetime plane for $\tau_{\tilde{\chi}_1^0} \lesssim 2$ ns.

PACS numbers: 13.85.Rm, 12.60.Jv, 13.85.Qk, 14.80.Ly

The standard model (SM) [1] of elementary particles has been enormously successful, but is incomplete. For theoretical reasons [2], and because of the observation of the '$ee\gamma\gamma$+missing transverse energy ($\not\!\!E_{\rm T}$)' [3, 4] candidate event by the CDF experiment during Run I at the Fermilab Tevatron, there is compelling rationale to search for the production and decay of new heavy particles that produce events with final state photons and $\not\!\!E_{\rm T}$ in collider experiments. Of particular theoretical interest are supersymmetry (SUSY) models with gauge-mediated SUSY-breaking (GMSB) [2]. Since many versions of these models have a similar phenomenology we consider the scenario in which the lightest neutralino ($\tilde{\chi}_1^0$) decays almost exclusively into a photon (γ) and a weakly interacting, stable gravitino ($\tilde{G}$) that gives rise to $\not\!\!E_{\rm T}$ by leaving a detector without depositing any energy [5]. The $\tilde{G}$ is a warm dark matter candidate, favored in these models to have 0.5 keV< $m_{\tilde{G}}$ <1.5 keV to be consistent with cosmological constraints [6]. Other direct searches [7–9] have constrained the mass of the $\widetilde{\chi}_1^0$ to have $m_{\widetilde{\chi}_1^0} \gtrsim 100$ GeV/c^2 for much of the parameter space. At the Tevatron, sparticle production is dominated by gaugino pairs, and the $\widetilde{\chi}_1^0$ mass ($m_{\widetilde{\chi}_1^0}$) and lifetime ($\tau_{\widetilde{\chi}_1^0}$) are the two most important parameters in determining the final states and their kinematics. Different search strategies are required for $\widetilde{\chi}_1^0$ lifetimes above and below about a nanosecond [10].

In this letter we describe a search for neutralinos that is sensitive to $\tau_{\widetilde{\chi}_1^0} \leq 2$ ns, favored for large $m_{\widetilde{\chi}_1^0}$, in which gaugino pairs are produced and decay to the $\gamma\gamma+\not\!\!E_{\rm T}+X$ final state where X are other high $E_{\rm T}$ final state particles. We use a dataset corresponding to an integrated luminosity of 2.6$\pm$0.2 fb^{-1} of $p\bar{p}$ collisions at $\sqrt{s} = 1.96$ TeV from the Tevatron collected with the CDF II detector [11]. This work improves previous Tevatron searches [7, 8] for GMSB in this channel by using an upgraded detector with a photon timing system [12], a larger data sample, and a new model of the $\not\!\!E_{\rm T}$ resolution (Met Model) [13]. The strategy is to select $\gamma\gamma$ candidates and search for the presence of both significant $\not\!\!E_{\rm T}$ and large total event transverse energy to indicate the decays of heavy gauginos. We perform an *a priori* analysis and optimize the selection criteria based on the expected sensitivity, taking into account the background and signal predictions.

A full description of the CDF Run II detector can be found elsewhere [11]. Here we briefly describe the aspects of the detector relevant to this analysis. The magnetic spectrometer consists of tracking devices inside a 3-m diameter, 5-m long superconducting solenoid magnet that operates at 1.4 T. A 3.1-m long drift chamber (COT) with 96 layers of sense wires is used to determine the momenta of charged particles, the z position of the $p\bar{p}$ interaction, and the time of the interaction. The calorimeter, constructed of projective towers, each with an electromagnetic (EM) and hadronic (HAD) compartment, is divided into a central barrel that surrounds the solenoid coil ($|\eta| < 1.1$) [3] and a pair of plug barrels that cover the region $1.1 < |\eta| < 3.6$. Both are used to identify photons, electrons, jets (j) [14] and $\not\!\!E_{\rm T}$ and measure their 4-momenta. The EM calorimeters are instrumented with a timing system, EMTiming [12], that measures the arrival time of photons.

Our analysis begins with events passing the three-level trigger, and the combined trigger selection [13] efficiency is effectively 100% efficient for our diphoton events. From this sample we create a subset of events with two photons with $|\eta| < 1.1$ and $E_{\rm T} > 13$ GeV. Offline, both photons are required to be in the fiducial part of the calorimeter and pass the standard CDF photon identification and isolation requirements [7] with two minor modifications to remove instrumental and electron backgrounds [13, 15].

This set of events is dominated by SM production of $\gamma\gamma$, γj with $j \rightarrow \gamma_{fake}$ and $jj \rightarrow \gamma_{fake}\gamma_{fake}$, where γ_{fake} is a jet misidentified as a photon. To minimize the number of these events with large $\not\!\!E_{\rm T}$ due to calorimeter energy mismeasurement we remove events if the $\not\!\!E_{\rm T}$ vector points along the direction, within $|\Delta\phi| < 0.3$, of the second photon or a narrow jet, with $E_{\rm T}^j > 5$ GeV and $|\eta| < 2.5$, located close to the calorimeter cracks at $\eta \sim 0$ and $|\eta| \sim 1.1$ [13]. To help maintain the projective nature of the photon reconstruction in the calorimeter we require a vertex with $|z_{\rm vertex}| < 60$ cm, which also helps to reduce non-collision backgrounds. For events with multiple reconstructed vertices we pick the vertex with the highest $\sum_{\rm tracks} p_T$ [3], unless assigning the photons to a different vertex lowers the $\not\!\!E_{\rm T}$, in which case we choose that vertex.

Non-collision backgrounds coming from cosmic rays and beam-related effects can produce $\gamma\gamma+\not\!\!E_{\rm T}$ candidates, and are removed from the inclusive $\gamma\gamma$ sample using a number of techniques. Photon candidates from cosmic rays are not correlated in time with collisions. We reject events if either photon is inconsistent with being from the collision [13]. Photon candidates can also be produced by beam-related muons that originate upstream of the detector (mostly from the more intense p beam) and travel through the calorimeter, typically depositing small amounts of energy near $\phi \approx 0$ for geometrical reasons. These are suppressed using standard beam halo identification requirements [15]. A total of 38,053 inclusive diphoton candidate events are dominated by SM backgrounds with fake $\not\!\!E_{\rm T}$.

Backgrounds to the $\gamma\gamma+\not\!\!E_{\rm T}$ final state come from SM production where $\not\!\!E_{\rm T}$ arises due to energy mismeasurements in the calorimeter or event reconstruction pathologies. To select events with real and significant $\not\!\!E_{\rm T}$, as part of the optimization, and to predict the contribution of SM backgrounds with mismeasured ("fake") $\not\!\!E_{\rm T}$ due to normal energy measurement fluctuations, we use a Met Model [13]. This model considers the clustered (jets) and unclustered energy in the event and calculates a probability for fluctuations in the energy measurement to produce $\not\!\!E_T^{fluct}$ equivalent to or larger than the measured $\not\!\!E_{\rm T}$ ($P_{\not\!\!E_T^{fluct} > \not\!\!E_{\rm T}}$). This probability is then used to define a $\not\!\!E_{\rm T}$-significance as $-\log_{10}\left(P_{\not\!\!E_T^{fluct} > \not\!\!E_{\rm T}}\right)$. Events with true and fake $\not\!\!E_{\rm T}$ of the same value should have, on average, different $\not\!\!E_{\rm T}$-significance. To estimate the expected $\not\!\!E_{\rm T}$-significance distribution for SM events with fake $\not\!\!E_{\rm T}$, and the number of mismeasured events above a given $\not\!\!E_{\rm T}$-significance requirement, we use pseudo-experiments where we smear the jets and unclustered energy, using appropriate resolution functions in the event. The systematic uncertainty is evaluated by comparing the Met Model predictions with a default set of parameters of the resolution functions to predictions obtained with parameters varied by one standard deviation.

Event reconstruction pathologies in SM events with no intrinsic $\not\!\!E_{\rm T}$, such as a wrong choice of the primary interaction vertex or tri-photon events with a lost photon, are unaccounted for by the Met Model. To obtain the prediction for this background we model SM kinematics and event reconstruction using a PYTHIA [16] $\gamma\gamma$ sample with a detector simulation [17] and normalize to the number of events in the inclusive $\gamma\gamma$ data sample to take into account γj and jj contributions to the backgrounds. We subtract the expectations for energy mismeasurement fluctuations in the MC to avoid double counting. The systematic uncertainties for this background prediction includes the uncertainty due to MC-data differences in the unclustered energy parameterization and on the jet energy scale.

Electroweak production of W's and Z's which decay to leptons can also give rise to the $\gamma\gamma+\not\!\!E_{\rm T}$ signature where one or more of the photons can be fake, but the $\not\!\!E_{\rm T}$ is due to one or more neutrinos. To estimate the contribution from these backgrounds we use MC simulations [17], normalized to their production cross sections and considering all the leptonic decay modes of the bosons. The Baur MC [18] is used to simulate $W\gamma$ and $Z\gamma$ production and decay where initial and final state radiation (ISR/FSR) simulates $W/Z+\gamma\gamma$ events. The PYTHIA [16] MC is used to simulate W, Z, with photons from ISR/FSR removed, and $t\bar{t}$ backgrounds where both photon candidates are fakes. To minimize the dependence of our predictions on potential Data-MC differences we scale our MC predictions to the observed number of $e\gamma$ events in data where we use the same diphoton triggers and analysis selection procedures as used for our inclusive $\gamma\gamma$ sample. Uncertainties are dominated by the $e\gamma$ normalization uncertainty.

Non-collision backgrounds are estimated using the data. Using the sample selection requirements, but requiring one of the photons to have $t_\gamma > 25$ ns we identify a cosmic enhanced sample. Similarly, we select a beam related background enhanced sample. We estimate the number of these events in the signal region, using the ratio of events outside the timing requirements to inside region and the measured efficiencies of the non-collision rejection requirements [13]. The uncertainties on both non-collision background estimates are dominated by statistical uncertainty on the number of identified events. Top of Figure 1 shows the $\not\!\!E_{\rm T}$-significance distribution for the inclusive $\gamma\gamma$ sample, along with shape of the predictions for all the backgrounds.

We estimate the sensitivity to heavy, neutral particles that decay to photons using the GMSB reference model [5] in the mass-lifetime range, $75 \leq m_{\tilde{\chi}_1^0} \leq 150$ GeV and $\tau_{\tilde{\chi}_1^0} \leq 2$ ns. Events from all SUSY processes [15] are simulated with PYTHIA [16] and followed by a detector simulation [17]. The acceptance is a strong function of the fraction of $\tilde{\chi}_1^0$ decays that occur in the detector volume, which is dependent on both $\tau_{\tilde{\chi}_1^0}$ and the masses of the sparticles, all of which scale linearly with $m_{\tilde{\chi}_1^0}$ for our model [10]. The total systematic uncertainty on the acceptance, after all kinematic requirements, is estimated to be 7%, dominated by the uncertainty on the photon ID efficiency (2.5% per photon). Other significant contributions come from uncertainties on ISR/FSR (4%), jet energy measurement (2%), $\not\!\!E_{\rm T}$-significance parameterizations (1%) and the parton distribution functions (1%).

We determine the kinematic selection requirements by optimizing the mean expected 95% confidence level (C.L.) cross section limit in the no-signal assumption without looking at the data in the signal region [19].

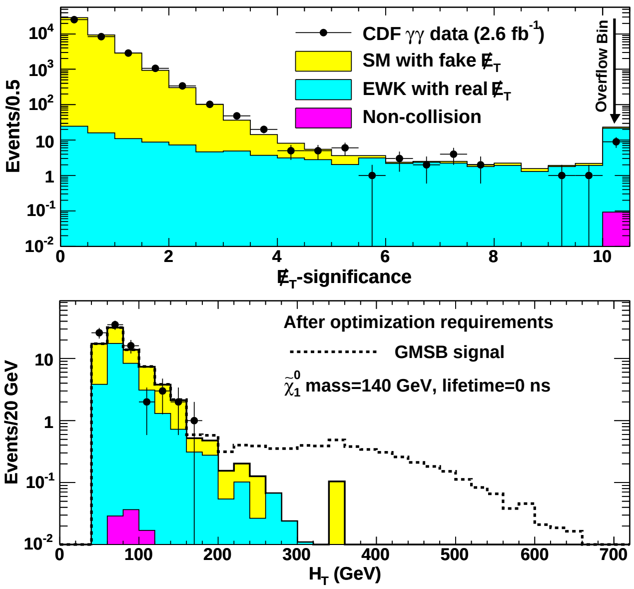

FIG. 1: The top plot shows the $\not\!\!E_{\rm T}$-significance prediction for the inclusive $\gamma\gamma$ candidate sample, along with the data. The bottom plot shows the predicted $H_{\rm T}$ (total $E_{\rm T}$ of photons, jets and $\not\!\!E_{\rm T}$) distribution after all but the final $H_{\rm T}$ requirement. There is no evidence for new physics and the data is well modeled by backgrounds alone.

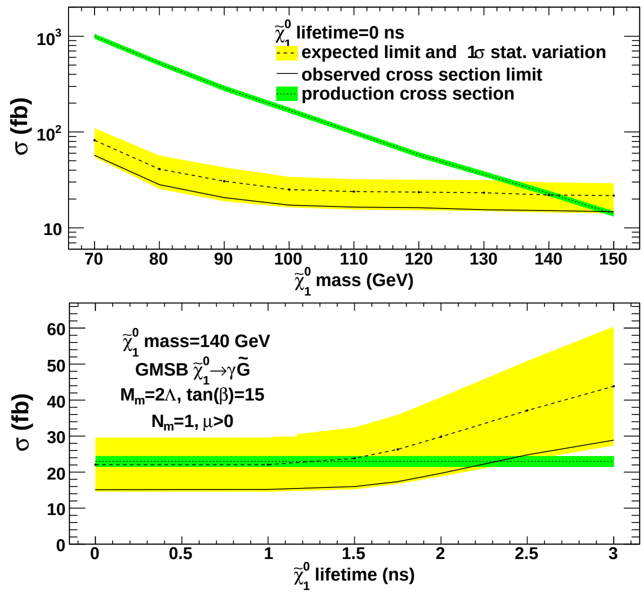

FIG. 2: The predicted and observed 95% C.L. cross section upper limits as a function of the $\tilde{\chi}_1^0$ mass at a lifetime of 0 ns (top) and as a function of the $\tilde{\chi}_1^0$ lifetime at a mass of 140 GeV/c^2 (bottom). Indicated in green (darker shading) is the production cross section, along with its 8.0% uncertainty-band. In yellow (lighter shading) is the RMS variation on the expected cross section limit.

To compute the predicted cross section upper limit we combine the luminosity, the acceptance and the background estimates with the systematic uncertainties using a Bayesian method [20]. The predicted limits are optimized by simultaneously varying the selection requirements for $\not\!\!E_{\rm T}$-significance, $H_{\rm T}$ (total $E_{\rm T}$ of photons, jets and $\not\!\!E_{\rm T}$), and the azimuthal angle between the two leading photons, $\Delta\phi(\gamma_1,\gamma_2)$. The large $\not\!\!E_{\rm T}$-significance requirement eliminates most of the SM background with fake $\not\!\!E_{\rm T}$. GMSB production is dominated by heavy gaugino pairs which decay to high $E_{\rm T}$, light final state particles via cascade decays. GMSB signal has, on average, larger $H_{\rm T}$ compared to SM backgrounds so that an $H_{\rm T}$ requirement can remove these backgrounds effectively. Electroweak backgrounds with large $H_{\rm T}$ typically consist of a high $E_{\rm T}$ photon recoiling against $W \rightarrow e\nu$, identified as $\gamma_{fake}\not\!\!E_{\rm T}$, which means the gauge boson decay is highly boosted. Thus, the two photon candidates in the final state are mostly back-to-back. Also, the high $E_{\rm T}$ diphotons with large H_T from SM background are mostly back-to-back with fake $\not\!\!E_{\rm T}$; the $\Delta\phi(\gamma_1,\gamma_2)$ cut, therefore, reduces both these backgrounds.

While each point in the considered $\tau_{\tilde{\chi}_1^0}$ vs. $m_{\tilde{\chi}_1^0}$ space gives a slightly different optimization, we choose a single set of requirements to maximize the expected 95% C.L. exclusion region; where the predicted production cross section at next-to-leading order [21] is above the expected cross section limit. The exclusion region also takes into account the production cross section uncertainties which are dominated by the parton distribution functions (7%) and the renormalization scale (3%). We find the optimal set of cuts, before unblinding the signal region, to be: $\not\!\!E_{\rm T}$-significance>3, $H_{\rm T} > 200$ GeV, and $\Delta\phi(\gamma_1,\gamma_2) < \pi - 0.35$ rad. With these requirements we predict 1.38±0.44 background events with 0.92±0.37 events from electroweak sources (dominated by $Z\gamma$ production) with real $\not\!\!E_{\rm T}$, 0.46±0.24 from SM with fake $\not\!\!E_{\rm T}$, and $0.001^{+0.008}_{-0.001}$ from non-collision sources.

No events in the data pass the final event selection. The acceptance for $m_{\tilde{\chi}_1^0} = 140$ GeV/c^2 and $\tau_{\tilde{\chi}_1^0} = 0$ ns is estimated to be 7.8±0.6%. The $H_{\rm T}$ distribution, normalized to expectations, is shown in Figure 1 (bottom), after all but the final $H_{\rm T}$ cut. The data is consistent with the no-signal hypothesis. We set cross section limits as a function of $m_{\tilde{\chi}_1^0}$ and $\tau_{\tilde{\chi}_1^0}$ respectively, as shown in Figure 2. The $m_{\tilde{\chi}_1^0}$ reach, based on the predicted and observed number of events for $\tau_{\tilde{\chi}_1^0} = 0$, is 141 GeV/c^2 and 149 GeV/c^2 respectively. These limits significantly extend the search sensitivity beyond the results of D0 [8] and, when combined with the complementary exclusions from CDF and LEP [9, 15], cover the region shown in Figure 3.

In conclusion, we have performed an optimized search for heavy, neutral particles that decay to photons in the $\gamma\gamma+\not\!\!E_{\rm T}$ final state using 2.6 fb^{-1} of data. There is no excess of events beyond expectations. We set cross section

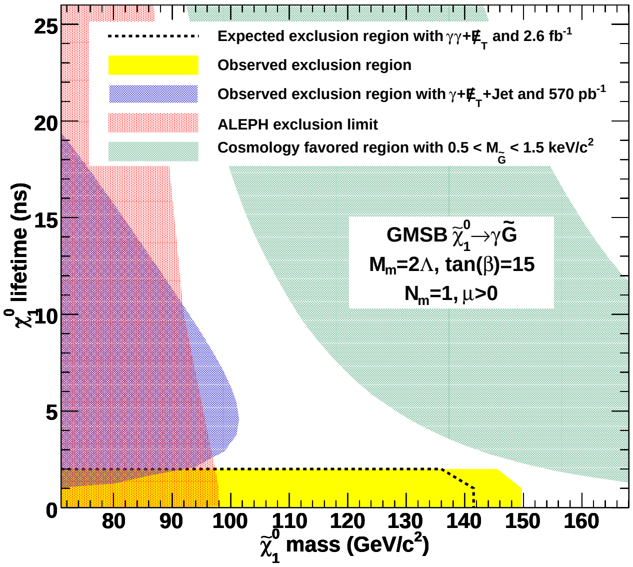

FIG. 3: The predicted and observed exclusion region along with the limit from ALEPH/LEP [9] and the CDF $\gamma+\not{E}_{\mathrm{T}}+jet$ 'delayed' photon analysis [15]. We have a mass reach of 141 GeV/c^2 (predicted) and 149 GeV/c^2 (observed) at lifetimes up to 1 ns. The shaded band shows the parameter space where $0.5 < m_{\tilde{G}} < 1.5$ keV/c^2, favored in cosmologically consistent models [6].

limits using a GMSB model with $\tilde{\chi}_1^0 \rightarrow \gamma\tilde{G}$, and find an exclusion region in the $\tau_{\tilde{\chi}_1^0}$-$m_{\tilde{\chi}_1^0}$ plane with a world-best 95% C.L. lower limit on the $\tilde{\chi}_1^0$ mass of 149 GeV/c^2 at $\tau_{\tilde{\chi}_1^0} = 0$ ns. By the end of Run II, an integrated luminosity of 10 fb^{-1} is possible for which we estimate a mass reach of $\simeq$ 160 GeV/c^2 at a lifetime of 0 ns by scaling the expected number of background events.

We thank the Fermilab staff and the technical staffs of the participating institutions for their vital contributions. This work was supported by the U.S. Department of Energy and National Science Foundation; the Italian Istituto Nazionale di Fisica Nucleare; the Ministry of Education, Culture, Sports, Science and Technology of Japan; the Natural Sciences and Engineering Research Council of Canada; the National Science Council of the Republic of China; the Swiss National Science Foundation; the A.P. Sloan Foundation; the Bundesministerium für Bildung und Forschung, Germany; the Korean Science and Engineering Foundation and the Korean Research Foundation; the Particle Physics and Astronomy Research Council and the Royal Society, UK; the Russian Foundation for Basic Research; the Comisión Interministerial de Ciencia y Tecnología, Spain; in part by the European Community's Human Potential Programme under contract HPRN-CT-2002-00292; and the Academy of Finland.

---

[1] See for example, F. Halzen and A. D. Martin, *Quarks and Leptons* (John Wiley & Sons, New York, 1984); C. Quigg, *Gauge Theories of the Strong, Weak, and Electromagnetic Interactions* (Addison-Wesley, Reading, MA, 1983); I. S. Hughes, *Elementary particles* (Cambridge University Press, Cambridge, England, 1990).

[2] S. Dimopoulos, S. Thomas, J. D. Wells, Nucl. Phys. B **488**, 39 (1997); S. Ambrosanio, G.D. Kribs and S.P. Martin, Phys. Rev. D **56**, 1761 (1997); G. F. Giudice and R. Rattazzi, Phys. Rept. **322**, 419 (1999); and S. Ambrosanio, G. Kane, G. Kribs, S. Martin and S. Mrenna, Phys. Rev. D **55**, 1372 (1997).

[3] We use a cylindrical coordinate system in which the proton beam travels along the z-axis, θ is the polar angle, ϕ is the azimuthal angle relative to the horizontal plane, and $\eta = -\ln\tan(\theta/2)$. The transverse energy and momentum are defined as $E_T = E\sin\theta$ and $p_T = p\sin\theta$ where E is the energy measured by the calorimeter and p the momentum measured in the tracking system. $\not{E}_{\mathrm{T}} = |-\sum_i E_T^i \vec{n_i}|$ where $\vec{n_i}$ is a unit vector that points from the interaction vertex to the i^{th} calorimeter tower in the transverse plane.

[4] F. Abe *et al.* (CDF Collaboration), Phys. Rev. Lett. **81**, 1791 (1998) and Phys. Rev. Lett **59**, 092002 (1999).

[5] B. C. Allanach *et al.*, Eur. Phys. J. C**25**, 113 (2002). We use benchmark model 8 and take the messenger mass scale $M_{\mathrm{mess}} = 2\Lambda$, $\tan(\beta) = 15$, $\mu > 0$ and the number of messenger fields $N_{\mathrm{mess}} = 1$. The $\tilde{G}$ mass factor and the supersymmetry breaking scale Λ are allowed to vary independently.

[6] C.-H. Chen and J. F. Gunion, Phys. Rev. D **58**, 075005 (1998).

[7] D. Acosta *et al.* (CDF Collaboration), Phys. Rev. D **71**, 031104 (2005).

[8] V.M. Abazov *et. al.* (D0 Collaboration), Phys. Lett. B **659**, 856 (2008).

[9] A. Heister *et al.* (ALEPH Collaboration), Eur. Phys. J. C **25**, 339 (2002); also see M. Gataullin, S. Rosier, L. Xia and H. Yang, arXiv:hep-ex/0611010; G. Abbiendi *et al.* (OPAL Collaboration), Proc. Sci. HEP2005 346 (2006); J. Abdallah *et al.* (DELPHI Collaboration), Eur. Phys. J. C **38** 395 (2005).

[10] D. Toback and P. Wagner, Phys. Rev. D **70**, 114032 (2004).

[11] D. Acosta *et al.* (CDF Collaboration), Phys. Rev. D **71**, 032001 (2005).

[12] M. Goncharov *et al.*, Nucl. Instrum. Methods A**565**, 543 (2006).

[13] T. Aaltonen *et al.*(CDF Collaboration), $\gamma\gamma + X$ Phys. Rev. D, to be submitted.

[14] For a description of how clusters of energy, for example $\tau^{\pm} \rightarrow \pi^{\pm}\pi^{\mp}\pi^{\pm}\nu_{\tau}$ decays, are identified as jets, see F. Abe *et al.*(CDF Collaboration), Phys. Rev. Lett. **68**, 1104 (1992). For a discussion of the jet energy measurements, see T. Affolder *et al.*(CDF Collaboration), Phys. Rev. D. **64**, 032001 (2001). For a discussion of standard jet correction systematics, see A. Bhatti *et al.*, Nucl. Instrum. Methods, A 566, 375 (2006). We use jets with cone size $\Delta R = 0.4$.

[15] A. Abulencia *et al.* (CDF Collaboration), Phys. Rev. Lett. **99**, 121801 (2007); T. Aaltonen

et al. (CDF Collaboration), Phys. Rev. D **78**, 032015 (2008).

[16] T. Sjöstrand *et al.*, Comput. Phys. Commun. **135**, 238 (2001). We use version 6.216.

[17] We use the standard GEANT based detector simulation [R. Brun *et al.*, CERN-DD/EE/84-1 (1987)] and add a parametrized EMTiming simulation.

[18] U. Baur, T Han and J. Ohnemus, Phys. Rev. D **48**, 5140 (1993); U. Baur, T Han and J. Ohnemus, Phys. Rev. D **57**, 2823 (1998); The $W\gamma$ and $Z\gamma$ processes are simulated using the leading-order event generator and have a k-factor fixed at 1.36. The initial and final state radiations (resulting in additional jets or photons), underlying event, and additional interactions are simulated by the PYTHIA Monte Carlo program [16].

[19] E. Boos, A. Vologdin, D. Toback, and J. Gaspard, Phys. Rev. D **66**, 013011 (2002).

[20] J. Conway, CERN Yellow Book Report No. CERN 2000-005, 2000, p. 247. We assume a flat prior in the production cross section.

[21] We use the leading-order cross sections generated by the PYTHIA [16] event generator and use the k-factors produced by PROSPINO 2.0 [W. Beenakker *et al.*, Phys. Rev. Lett. **83**, 3780 (1999)].